

Conference paper

UDC 538.958

DOI: <https://doi.org/10.18721/JPM.191.111>

## **Interband absorption and photoluminescence in lens-shaped quantum dots: an adiabatic approach**

**D.G. Gevorgyan**<sup>1</sup>□, **S.P. Gavalajyan**<sup>1,2</sup>, **M.Ya. Vinnichenko**<sup>3</sup>, **E.M. Kazaryan**<sup>1</sup>

<sup>1</sup>Russian-Armenian University, Yerevan, Armenia;

<sup>2</sup>Quantum Materials and Nanophotonics Laboratory,

A.B. Nalbandyan Institute of Chemical Physics, Yerevan, Armenia;

<sup>3</sup>Peter the Great St. Petersburg Polytechnic University, St. Petersburg, Russia

□ [davitgevorgyan2000@gmail.com](mailto:davitgevorgyan2000@gmail.com)

**Abstract.** We present an analytic-numerical framework for carriers and excitons in lens-shaped (semi-ellipsoidal) quantum dots within the effective-mass and envelope-function approximations, assuming hard-wall confinement. Exploiting the geometry, we use an adiabatic separation of fast (axial) and slow (planar) motion to obtain closed-form single-particle states and energies. The exciton binding energy is evaluated numerically in first-order perturbation theory using the analytic envelopes. Interband absorption follows from bright-state selection rules, and photoluminescence is obtained from absorption via the van Roosbroeck–Shockley relation with Lorentzian broadening. It is shown that single-particle confinement energies are much more sensitive to the dot height than to the lateral size, states with higher axial quantum number lie well above the lowest branch, the Coulomb binding decreases with increasing size, exhibiting comparable fractional sensitivity to both the axial and planar semi-axes and grouping primarily by radial quantum number. The framework yields compact formulas, transparent scaling trends, and interpretable spectra for the design and analysis of lens-shaped quantum dots.

**Keywords:** Quantum dots, lens-shaped quantum dots, exciton, photoluminescence

**Funding:** This work was supported by the Science Committee of the Republic of Armenia (Research project № 24AA-1C047). M.Y.V. acknowledges support from the Ministry of Science and Higher Education of the Russian Federation (State Assignment FSEG-2023-0016).

**Citation:** Gevorgyan D.G., Gavalajyan S.P., Vinnichenko M.Ya., Kazaryan E.M., Interband absorption and photoluminescence in lens-shaped quantum dots: an adiabatic approach, St. Petersburg State Polytechnical University Journal. Physics and Mathematics. 19 (1.1) (2026) 69–74. DOI: <https://doi.org/10.18721/JPM.191.111>

This is an open access article under the CC BY-NC 4.0 license (<https://creativecommons.org/licenses/by-nc/4.0/>)

Конференционная статья

УДК 538.958

DOI: <https://doi.org/10.18721/JPM.191.111>

## **Межзонное поглощение и фотолюминесценция в линзообразных квантовых точках: адиабатический подход**

**Д.Г. Геворгян**<sup>1</sup>□, **С.П. Гаваладжян**<sup>1,2</sup>, **М.Я. Винниченко**<sup>3</sup>, **Э.М. Казарян**<sup>1</sup>,

<sup>1</sup>Российско-Армянский университет, г. Ереван, Армения;

<sup>2</sup>Лаборатория квантовых материалов и нанопотоники, Институт химической физики им. А.Б. Налбандяна, г. Ереван, Армения;

<sup>3</sup>Санкт-Петербургский политехнический университет Петра Великого, Санкт-Петербург, Россия

□ [davitgevorgyan2000@gmail.com](mailto:davitgevorgyan2000@gmail.com)

**Аннотация.** Представлен аналитико-численный подход к описанию носителей и экситонов в линзовидных (полуэллипсоидальных) квантовых точках в рамках приближений эффективной массы и огибающей функции при предположении бесконечного потенциального ограничения. Используя геометрию системы, мы применяем адиабатическое разделение быстрых (аксиальных) и медленных (плоских) движений, что позволяет получить аналитические выражения для одночастичных состояний и энергий. Энергия связи экситона рассчитывается численно в первом порядке теории возмущений с использованием аналитических огибающих функций. Межзонное поглощение определяется правилами отбора для светлых состояний, а фотолюминесценция получается из спектра поглощения с помощью соотношения ван Роосбрука–Шокли с лоренцевским уширением. Показано, что одночастичные энергии значительно более чувствительны к высоте квантовой точки, чем к ширине; состояния с более высоким аксиальным квантовым числом располагаются значительно выше нижней ветви спектра; кулоновская энергия связи уменьшается с ростом размеров структуры, демонстрируя сопоставимую относительную чувствительность как к аксиальной, так и к плоской полуосям и группируясь преимущественно по радиальному квантовому числу. Предложенный подход приводит к компактным формулам, наглядным закономерностям масштабирования и физически интерпретируемым спектрам, что делает его удобным инструментом для анализа и проектирования линзовидных квантовых точек.

**Ключевые слова:** квантовые точки, линзообразные квантовые точки, экситон, фотолюминесценция

**Финансирование:** Работа выполнена при поддержке Комитета по науке Республики Армения (научный проект № 24АА-1С047). М. Я. В. выражает благодарность Министерству науки и высшего образования Российской Федерации за поддержку в рамках государственного задания FSEG-2023-0016.

**Ссылка при цитировании:** Геворгян Д.Г., Гаваладжян С.П., Винниченко М.Я., Казарян Э.М. Межзонное поглощение и фотолюминесценция в линзообразных квантовых точках: адиабатический подход // Научно-технические ведомости СПбГПУ. Физико-математические науки. 2026. Т. 19. № 1.1. С. 69–74. DOI: <https://doi.org/10.18721/JPM.191.111>

Статья открытого доступа, распространяемая по лицензии CC BY-NC 4.0 (<https://creativecommons.org/licenses/by-nc/4.0/>)

## Introduction

Semiconductor quantum dots (QDs) are often described as “artificial atoms” because quantum confinement yields discrete energy spectra and size-tunable optical properties with broad impact across imaging, sensing, and optoelectronics. Recent surveys and application-driven studies highlight both the technological progress and remaining challenges in materials, devices, and integration [1]. In bioimaging and biodiagnostics, QDs offer bright, photostable labels with multiplexing capabilities [2]. Together, these works underscore the central role of QDs in modern photonics and the importance of tractable theoretical models that connect geometry to spectra.

Beyond composition and overall size, shape is a powerful design parameter for tailoring selection rules, oscillator strengths, and polarization characteristics. Ellipsoidal families – including oblate and prolate spheroids – have been analyzed in detail for their electronic states and interband absorption [3, 4], as well as for related ellipsoidal/lens-like nanostructures with strong shape anisotropy [5 – 7]. In epitaxial systems, lens-shaped (semi-ellipsoidal) QDs arise naturally. Related work on asymmetric biconvex lens-shaped dots mapped the influence of external fields on interband and intraband optical properties [8].

Against this backdrop, the present paper develops a minimal effective-mass, envelope-function description for carriers and excitons in lens-shaped (semi-ellipsoidal) QDs with hard-wall confinement. We derive closed-form single-particle states in an adiabatic (fast/slow) separation, compute first-order Coulomb corrections to exciton energies using analytic envelopes, and obtain interband absorption together with photoluminescence (PL) via the van Roosbroeck–Shockley

detailed balance relation [9]. Our goal is to provide compact formulas, transparent scaling trends, and interpretable spectra that clarify how lens geometry organizes bright transitions and Coulomb-induced splittings.

### Theory

**Single-Particle Energies and States.** The geometry of the lens-shaped quantum dot is modeled by a cylindrically symmetric semi-ellipsoid illustrated in Fig. 1 that satisfies the condition  $c \ll a$  where  $a$  and  $c$  denote the major and minor semi-axes of the semi-ellipsoid, respectively.

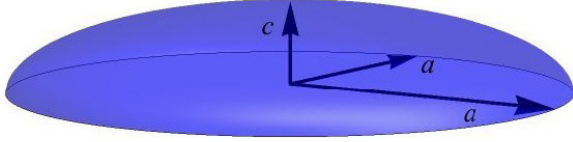


Fig. 1. Schematic representation of a semi-ellipsoid with semi-axes  $a$ ,  $a$  and  $c$

The confining potential of a particle in such a quantum dot is defined as  $V(\mathbf{r}) = 0$  inside and  $V(\mathbf{r}) = \infty$  outside the dot. The single-particle Hamiltonian in cylindrical coordinates then takes the form

$$\hat{H} = -\left(\frac{\partial^2}{\partial r^2} + \frac{1}{r} \frac{\partial}{\partial r} + \frac{1}{r^2} \frac{\partial^2}{\partial \varphi^2} + \frac{\partial^2}{\partial z^2}\right) + V(\mathbf{r}), \quad (1)$$

where distances and energies are expressed in effective atomic units (Bohr radius and Rydberg).

It follows from the condition  $c \ll a$  that the motion of the particle along the  $OZ$  axis is much faster than in the  $OXY$  plane, which makes it possible to apply the adiabatic approximation. Within this approximation, the particle Hamiltonian can be separated into two components:  $\hat{H}_r$  corresponds the slow planar degrees of freedom, while  $\hat{H}_z$  corresponds to the fast axial one. The solution of the stationary Schrödinger equation is sought in the form

$$\Psi(r, \varphi, z) = \Psi_r(r) \Psi_z(r, z) e^{im\varphi}. \quad (2)$$

For a fixed value of  $r$ , the fast subsystem can be represented as a potential well with an effective width  $w(r) = c\sqrt{1-r^2/a^2}$  and the solution of the Schrödinger equation yields

$$\Psi_z(r, z) = \sqrt{\frac{2}{w(r)}} \sin\left(\frac{\pi n_z z}{w(r)}\right), \quad \varepsilon_z(r) = \frac{\pi^2 n_z^2}{w^2(r)}, \quad (3)$$

where  $n_z$  is the axial quantum number. Here  $\varepsilon_z(r)$  can be expanded in a Taylor series with respect to  $r/a$  as

$$\varepsilon_z(r) \approx \alpha n_z^2 + \beta^2 n_z^2 r^2, \quad \alpha = \frac{\pi^2}{c^2}, \quad \beta = \frac{\pi}{ac}. \quad (4)$$

Substituting  $\varepsilon_z(r)$  into the equation for the slow subsystem as an effective potential leads to the problem of a two-dimensional harmonic oscillator. Accordingly, the radial component of the wave function  $\Psi_r(r)$  is given by

$$\Psi_r(r) = A r^{|m|} e^{-\beta n_z r^2/2} L_{n_r}^{|m|}(\beta n_z r^2), \quad (5)$$

where  $n_r$  and  $m$  are the radial and angular quantum numbers, respectively,  $L_{n_r}^{|m|}(\cdot)$  is the associated Laguerre polynomial, and  $A$  is a normalization constant.

The corresponding single-particle energy spectrum is

$$E_{n_z, n_r, m} = \alpha n_z^2 + \beta n_z (2n_r + |m| + 1). \quad (6)$$

For the lowest longitudinal branch  $n_z = 1$ , the energy depends only on  $N \equiv 2n_r + |m|$ ; all states with the same  $N$  are degenerate with multiplicity  $N + 1 = 2n_r + |m| + 1$ .

### Exciton Energy

The Hamiltonian of the exciton is

$$\hat{H} = \hat{H}_e + \hat{H}_h - \frac{1}{|\mathbf{r}_e - \mathbf{r}_h|}, \quad (7)$$

where  $\hat{H}_e$  and  $\hat{H}_h$  are the single-particle Hamiltonians of the electron and hole, respectively, and the last term describes their Coulomb attraction.

When comparing with optical spectra, the relevant interband transition energy includes the band gap  $E_g$ :

$$E_{ex} = E_g + E_{eh}, E_{eh} = E_e + E_h - V_{eh}, \quad (8)$$

where  $E_e$  and  $E_h$  are the confinement (single-particle) energies of the electron and the hole measured from the band edges, and

$$V_{eh} = \int \psi_e^*(\mathbf{r}_e) \psi_h^*(\mathbf{r}_h) \frac{1}{|\mathbf{r}_e - \mathbf{r}_h|} \psi_e(\mathbf{r}_e) \psi_h(\mathbf{r}_h) d^3\mathbf{r}_e d^3\mathbf{r}_h, \quad (9)$$

where  $\psi_{e,h}$  are the normalized envelopes from the previous subsection.

### Interband Absorption and Photoluminescence

Interband absorption probes the allowed optical transitions in the quantum dot and is strongly shaped by excitonic effects. The absorption coefficient (up to a material-dependent prefactor) can be written as a sum over electron-hole envelope states. Taking into account the orthonormality of the modes, it can be reduced to a sum over bright transitions only ( $n_z^e = n_z^h, n_r^e = n_r^h, m_e = -m_h$ ),

$$\alpha(\hbar\omega) \propto \sum_{n_r, n_z, m} \delta[\hbar\omega - E_{ex}(n_r, n_z, m)]. \quad (10)$$

Substituting the absorption spectrum into the RS relation [10] yields the PL spectrum

$$R(\hbar\omega) \propto (\hbar\omega)^2 \sum_{n_r, n_z, m} \delta(\hbar\omega - E_{ex}(n_r, n_z, m)) \frac{f_c(1-f_v)}{f_v - f_c}. \quad (11)$$

where  $f_c$  and  $f_v$  are the Fermi-Dirac occupation probabilities of the conduction and valence band states that depend on the lattice temperature.

In practice, delta-peaks are broadened by coupling to phonons. A convenient replacement is a Lorentzian with typical half-width at half-maximum  $\gamma$  in the range 0.5–5 meV. The resulting broadened spectra are evaluated numerically in the next section.

### Results and Discussion

Fig. 2 shows the probability density  $|\psi_{n_z, n_r, m}(r, \varphi, z)|^2$  for several representative states in the lens-shaped dot. The expected nodal structure is evident: along  $z$  there are  $n_z - 1$  internal nodes and  $n_z$  lobes, while in the radial direction the Laguerre part yields exactly  $n_r$  radial nodes. The angular quantum number  $m$  controls the central behavior via the  $r^{|m|}$  term: for  $m = 0$  the density is maximal at  $r = 0$ , whereas for  $|m| \leq 1$  it vanishes at  $r = 0$  and forms ring-like maxima whose radius grows with  $|m|$ . Overall, the examples show clear localization of the particle near the dot center for the lowest  $(n_r, m)$  and the emergence of additional nodes as  $n_z$  or  $n_r$  increase.

States with  $n_z > 1$  have energies far above the  $n_z = 1$  ones as a direct consequence of the relation  $c \ll a$ , and will be disregarded in what follows. The lowest level shows only a very weak dependence on  $a$  since the dominant  $\alpha$ -term is controlled solely by  $c$ .

Fig. 3 presents the electron-hole Coulomb contribution  $V_{eh}$  in electron Rydbergs for several  $n_z = 1$  states as a function of the dot dimensions. The range is chosen based on GaAs parameters. As either the height  $c$  (a) or the lateral semi-axis  $a$  (b) increases, the binding weakens monotonically. Notably, the sensitivity to relative changes in  $a$  and in  $c$  is comparable over the plotted ranges. An interesting systematic ordering emerges: curves group primarily by the radial quantum number  $n_r$  (across different  $m$ ) and with an increasing  $n_r$  the binding energy decreases.

The calculated PL spectrum  $R(\hbar\omega)$  for the representative dot is shown in Fig. 4. The sequence of peaks follows the ordering of the single-particle ladder corrected by the electron-hole attraction consistent with the selection rules. In the non-interacting limit, the states within a fixed  $N \equiv 2n_r + |m|$  would be degenerate with multiplicity  $N + 1$ . The Coulomb term  $V_{eh}$  depends on  $(n_r, |m|)$  and therefore partially lifts this degeneracy.

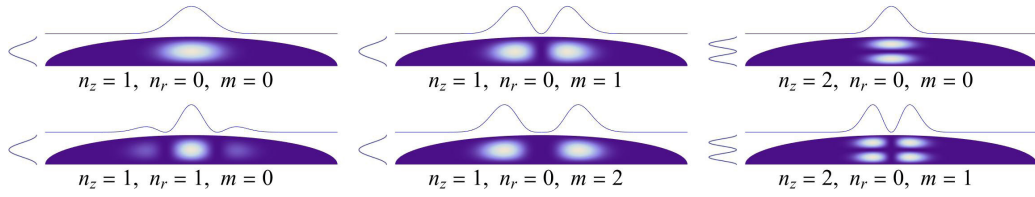


Fig. 2. Probability densities and marginals in the lens-shaped dot. Each panel displays the probability density  $|\psi_{n_z, n_r, m}(r, \phi, z)|^2$  for a representative state. For each state, curves plotted to the left and on top show the longitudinal and the radial marginal probability densities respectively

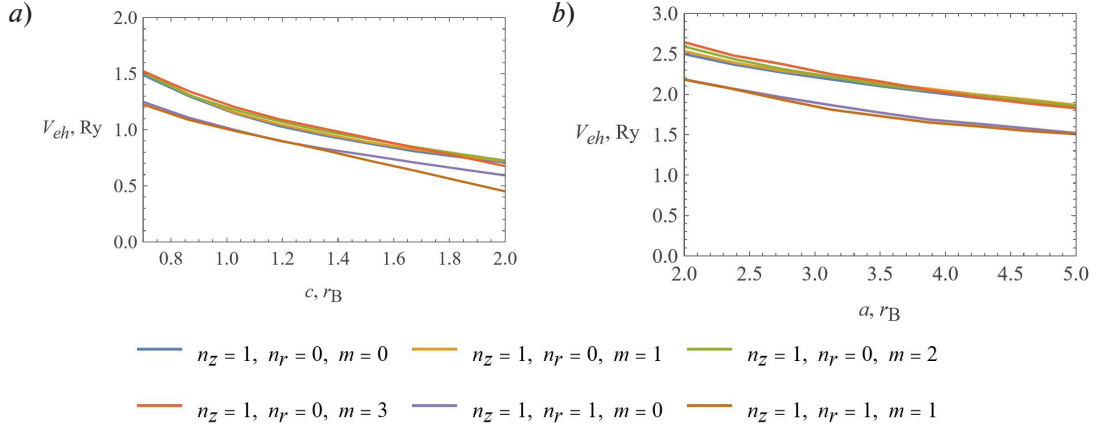


Fig. 3. Exciton Coulomb binding energy versus vertical semi-axis  $c$  at fixed  $a = 5r_B$  (a) and lateral semi-axis  $a$  at fixed  $c = 0.5r_B$  (b) for  $n_z = 1$

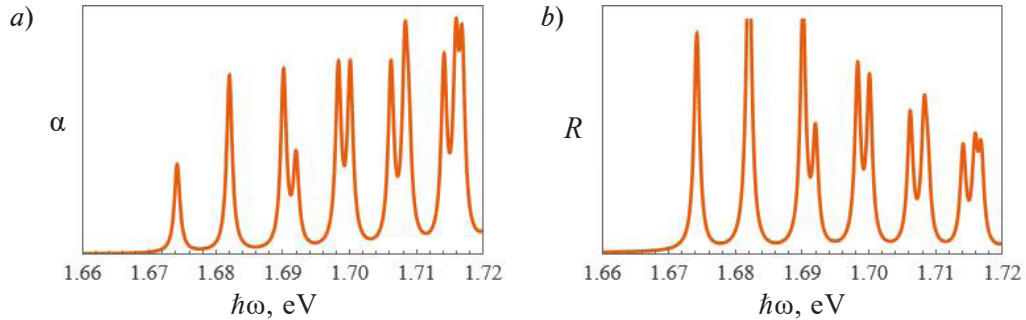


Fig. 4. Absorption (a) and photoluminescence (b) spectra for a GaAs lens-shaped dot with  $a = 5r_B$  and  $c = 0.5r_B$  and  $T = 300\text{K}$ . Both graphs use Lorentzian peak broadening with half-width  $\gamma = 0.5\text{meV}$

### Conclusion

We developed an analytic-numerical framework for carriers and excitons in a lens-shaped (semi-ellipsoidal) quantum dot with hard-wall confinement. Within an adiabatic separation of fast (longitudinal) and slow (in-plane) motion, we derived closed-form envelope functions and the single-particle spectrum, and established simple size dependence. Using these states, we evaluated the electron-hole interaction energy and constructed interband absorption and PL spectra.

The main findings are as follows. (i) The Coulomb binding  $|V_{eh}|$  decreases monotonically with increasing  $a$  or  $c$ ; over the plotted ranges, its relative sensitivity to changes in  $a$  and  $c$  is comparable, and the curves group primarily by the radial quantum number  $n_r$ , reflecting the role of central localization. (ii) The absorption and PL spectra are dominated by bright transitions with matched envelope quantum numbers; electron-hole attraction lifts the non-interacting degeneracy within each  $N = 2n_r + |m|$  multiplet, shifting more localized states to lower energy and producing the observed multiplet structure.

In summary, the semi-ellipsoidal model combined with adiabatic separation provides compact analytic states, clear size-dependence trends, and physically interpretable optical spectra, offering a useful baseline for both the design and analysis of lens-shaped quantum dots.

## REFERENCES

1. **García de Arquer, F.P., Talapin D.V., Klimov V.I., Arakawa Y., Bayer M., Sargent E.H.**, Semiconductor quantum dots: Technological progress and future challenges, *Science*. 373 (6555) (2021) eaaz8541.
2. **Skolnick M.S., Mowbray D.J.**, Self-assembled semiconductor quantum dots: Fundamental physics and device applications. *Annu. Rev. Mater. Res.* 34 (1) (2004) 181–218.
3. **Baghdasaryan D.A., Hayrapetyan D.B., Kazaryan E.M.**, Oblate spheroidal quantum dot: electronic states, direct interband light absorption and pressure dependence, *The European Physical Journal B*. 88 (9) (2015) 223.
4. **Baghdasaryan D.A., Hayrapetyan D.B., Kazaryan E.M.**, Prolate spheroidal quantum dot: electronic states, direct interband light absorption and electron dipole moment, *Physica B: Condensed Matter*. 479 (2015) 85–89.
5. **Hayrapetyan D.B., Dvovyan K.G., Kazaryan E.M.**, Direct interband light absorption in a strongly oblated ellipsoidal quantum dot, *Journal of Contemporary Physics (Armenian Academy of Sciences)*. 42 (4) (2007) 151–157.
6. **Baghdasaryan D.A., Hayrapetyan D.B., Kazaryan E.M.**, Optical properties of narrow band prolate ellipsoidal quantum layers ensemble, *Journal of Nanophotonics*. 10 (3) (2016) 033508–033508.
7. **Hayrapetyan D.B., Ohanyan G.L., Baghdasaryan D.A., Sarkisyan H.A., Baskoutas S., Kazaryan E.M.**, Binding energy and photoionization cross-section of hydrogen-like donor impurity in strongly oblate ellipsoidal quantum dot, *Physica E: Low-dimensional Systems and Nanostructures*. 95 (2018) 27–31.
8. **Mkrtchyan M.A., Hayrapetyan D.B., Kazaryan E.M., Sarkisyan H.A., Vinnichenko M.Y., Shalygin V.A., Firsov D.A., Petrosyan L.S.**, Effects of an external magnetic field on the interband and intraband optical properties of an asymmetric biconvex lens-shaped quantum dot, *Nanomaterials*. 12 (1) (2021) 60.
9. **Bhattacharya R., Pal B., Bansal B.**, On conversion of luminescence into absorption and the van Roosbroeck–Shockley relation. *Applied Physics Letters*. 100 (22) (2012) 222103.

## THE AUTHORS

**GEVORGYAN Davit G.**  
davitgevorgyan2000@gmail.com  
ORCID: 0009-0004-0202-4396

**GAVALAJYAN Sargis P.**  
sargis.gavalajyan@rau.am  
ORCID: 0009-0002-2353-1704

**VINNICHENKO Maxim Ya.**  
mvin@spbstu.ru  
ORCID: 0000-0002-6118-0098

**KAZARYAN Eduard M.**  
edghaz@mail.ru

*Received 15.12.2025. Approved after reviewing 09.02.2026. Accepted 18.02.2026.*